Journal of Biomedical Optics

BiomedicalOptics.SPIEDigitalLibrary.org

Delayed luminescence to monitor programmed cell death induced by berberine on thyroid cancer cells

Agata Scordino
Agata Campisi
Rosaria Grasso
Roberta Bonfanti
Marisa Gulino
Liliana Iauk
Rosalba Parenti
Francesco Musumeci

SPIE.

Delayed luminescence to monitor programmed cell death induced by berberine on thyroid cancer cells

Agata Scordino,[a,b,*] Agata Campisi,[c] Rosaria Grasso,[b] Roberta Bonfanti,[c] Marisa Gulino,[d,b] Liliana Iauk,[e] Rosalba Parenti,[e] and Francesco Musumeci[a,b]
[a]University of Catania, Department of Physics and Astronomy, via Santa Sofia 64, Catania I95123, Italy
[b]Southern National Laboratories of National Institute for Nuclear Physics, via Santa Sofia 62, Catania I95123, Italy
[c]University of Catania, Department of Drugs Science, viale Andrea Doria 6, Catania I95125, Italy
[d]"Kore" University, Faculty of Engineering, Architecture and Physical Education, Via delle Olimpiadi, Enna I94100, Italy
[e]University of Catania, Department of Bio-Medical Science, viale Andrea Doria 6, Catania I95125, Italy

Abstract. Correlation between apoptosis and UVA-induced ultraweak photon emission delayed luminescence (DL) from tumor thyroid cell lines was investigated. In particular, the effects of berberine, an alkaloid that has been reported to have anticancer activities, on two cancer cell lines were studied. The FTC-133 and 8305C cell lines, as representative of follicular and anaplastic thyroid human cancer, respectively, were chosen. The results show that berberine is able to arrest cell cycle and activate apoptotic pathway as shown in both cell lines by deoxyribonucleic acid fragmentation, caspase-3 cleavage, p53 and p27 protein overexpression. In parallel, changes in DL spectral components after berberine treatment support the hypothesis that DL from human cells originates mainly from mitochondria, since berberine acts especially at the mitochondrial level. The decrease of DL blue component for both cell lines could be related to the decrease of intra-mitochondrial nicotinamide adenine dinucleotide and may be a hallmark of induced apoptosis. In contrast, the response in the red spectral range is different for the two cell lines and may be ascribed to a different iron homeostasis. [DOI: 10.1117/1.JBO.19.11.117005]

Keywords: apoptosis; berberine; delayed luminescence; mitochondria; cancer cells; human thyroid cells.

Paper 140484R received Jul. 31, 2014; accepted for publication Oct. 17, 2014; published online Nov. 13, 2014.

1 Introduction

Nowadays, growing interest has been shown in the possibility of using noninvasive diagnostic tools in clinical survey. In this respect, detection of ultraweak biophoton emission makes it possible to acquire immediate information on biological activities noninvasively.[1,2] Delayed luminescence (DL), which is the prolonged (usually in microsecond to second time scale) ultraweak emission of optical photons from a biological sample after the illumination source was switched off, has been investigated in order to distinguish between tumor and normal fibroblasts,[3–6] or to assess the proapoptotic capacity of combined cancer treatments.[7]

Biomolecules inside cells can act as endogenous fluorophores (autofluorescence) when excited by UV/Vis radiation of suitable wavelength. The majority of cell autofluorescence originates from mitochondria and lysosomes[8] and changes occurring in the cell state during physiological and/or pathological processes result in modifications of both amount and distribution of endogenous fluorophores, as well as of the chemical-physical properties of their microenvironment. Among the major molecules that have been identified to contribute in autofluorescence signal from biological tissue,[8–10] nicotinamide adenine dinucleotide (NADH, free and bound form) emits in the blue region (emission bands peaking in the range 444 to 460 nm), flavins and lipopigments emit in the yellow region (emission peaks at 520 and 570 nm, respectively) and protoporphyrin emits in the red region (emission bands peaking in the range 630 to 710 nm) of the spectrum.

The role of several natural biomarkers in cancer research has been widely studied[9–14] by also demonstrating the mitochondrial origin of the luminescence.[15–17] In fact, progress over the past few years has led to the recognition that, in addition to their established role in generating energy for the cell, mitochondria play a key role into the intrinsic pathway for programmed cell death[18] by releasing cytochrome *c* into the cytosol, thereby activating caspases. With a few exceptions, mitochondria represent an essential component of many apoptotic pathways.[19]

It has been reported that berberine, an alkaloid extracted from rhizomes and roots of plants such as the Berberis, Coptis, and Hydrastis species extensively used in Chinese traditional medicine,[20,21] was able to block the cell cycle of a large variety of tumor cells also activating the apoptotic pathway. Several mechanisms involved in berberine's antitumor activity have been identified, including cytochrome *c* release, caspase-3 cleavage, cell cycle arrest, and deoxyribonucleic acid (DNA) fragmentation.[22–25] Furthermore, data from mouse melanoma cells showed that berberine is selectively accumulated by mitochondria.[26]

Recently, the relationship between apoptosis and DL of leukemia Jurkat T-cells was investigated[7,27] under a variety of treatments, among them flavonoids that preferentially target malignant cells by inhibiting cell proliferation and inducing apoptosis. The role of mitochondrial respiratory Complex I in DL emission was also pointed out.[28]

In this paper, we assessed the correlation between apoptosis and UVA-induced ultraweak photon emission (DL) in two cell lines, the human follicular (FTC-133) and anaplastic (8305C)

*Address all correspondence to: Agata Scordino, E-mail: scordino@lns.infn.it

0091-3286/2014/$25.00 © 2014 SPIE

human thyroid cancer cell lines, as representatives of two aggressive types of thyroid cancer, poorly differentiated, and dedifferentiated, respectively. The effect of berberine on FTC-133 and 8305C human thyroid cancer cell lines was also investigated in order to correlate biological observation with physical parameters. According to the results reported in the literature,[22–25] the effect of the alkaloid on the activation of apoptotic pathway was evaluated by testing caspase-3 cleavage and DNA fragmentation, and the effect on cell cycle progression was also evaluated by testing p53 and p27 proteins' overexpression. In parallel, DL spectroscopy changes, before and after berberine treatment, were evaluated and compared.

2 Materials and Methods

2.1 *Materials*

Follicular (FTC-133) and anaplastic (8305C) human thyroid cancer cell lines were purchased from Cell Bank Interlab Cell Line Collection (Genoa, Italy). Dulbecco's modified eagle medium (DMEM) and minimum essential medium (MEM) containing 2-mM GlutaMAX (GIBCO), Ham's F12 (GIBCO), nonessential amino acids, heat-inactivated fetal bovine serum (FBS, GIBCO), normal goat serum (NGS, GIBCO), streptomycin and penicillin antibiotics, 0.05% trypsin-EDTA solution were from invitrogen (Milan, Italy). Aprotinin, leupeptin, pepstatin, Lab-Tek chamber slides II, 3(4,5-dimethyl-thiazol-2-yl)2,5-diphenyl-tetrazolium bromide salts (MTT), berberine hydrochloride, and other analytical chemicals were obtained from Sigma–Aldrich (Milan, Italy). Mouse monoclonal antibody against caspase-3 was purchased from Becton, Dickinson (Milan, Italy). Mouse monoclonal antibodies against p27 and β-tubulin were purchased from Chemicon (Prodotti Gianni, Milan, Italy). Mouse monoclonal antibody against p53 was purchased from Santa Cruz-Biotechnologies (USA). Horseradish peroxidase (HRP)-conjugated anti-mouse IgG was from Amersham Pharmacia Biotech (Milan, Italy). Enhanced chemiluminescence (ECL) developing system for immunoblots was purchased from Santa Cruz Biotechnology Inc. (Santa Cruz, CA, USA). ApoAlert DNA fragmentation assay kit was purchased from Clonteck (Milan, Italy).

2.2 *Methods*

2.2.1 *Cell cultures*

FTC-133 and 8305C cell lines were suspended in appropriate culture medium and plated in flasks (75 cm^2) at a final density of 2×10^6 cells/flask or in Lab-Tek chamber slides II (4 wells, well volume 1 mL) at a final density 0.5×10^5 cells/well. In particular, FTC-133 cells were suspended in DMEM containing 2-mM Gluta-MAX, 10% FBS, streptomycin (50 μg/mL), penicillin (50 U/mL). 8305C cells were suspended in MEM containing 2-mM Gluta-MAX, 10% FBS, streptomycin (50 μg/mL), penicillin (50 U/mL), and 1% nonessential amino acids. Cells were incubated at 37°C in a humidified 5% CO_2–95% air mixture. The medium was replaced every 2 or 3 days. When the cultures were about 85% to 90% confluent, cells were suspended by using 0.05% trypsin and 0.53-mM EDTA solution for 5 min at 37°C in humidified 5% CO_2–95% air mixture. Trypsinization was stopped by adding to the cell cultures 20% FBS. Cells were centrifuged at 200 × g for 10 min, the pellets were suspended in appropriate culture medium and plated in flasks at 1:4 density ratio. Finally, cell cultures were incubated at 37°C in humidified 5% CO_2–95% air mixture, and the medium was replaced every 2 or 3 days.

2.2.2 *Berberine hydrochloride treatment*

FTC-133 and 8305C cells were plated at a final density of 1×10^4 cells/mL, and fed in fresh complete medium. In preliminary experiments, we incubated the cultures both in the absence and in the presence of berberine hydrochloride at different concentrations (5, 10, 25, 50, and 100 μg/mL) for 12, 24, and 48 h, in order to establish the optimal value for alkaloid concentration and exposure time. For this purpose, MTT test and morphological characterization were utilized.[29]

2.2.3 *MTT bioassay*

To monitor cell viability untreated or berberine hydrochloride-treated FTC-133 and 8305C cell cultures were set up to 60×10^4 cells/well of a 96-multiwell flat-bottomed 200-μL microplates.[29] Cells were incubated at 37°C in a humidified 5% CO_2–95% air mixture. At the end of treatment time, 20 μl MTT salts, 0.5% in phosphate buffer saline, were added to every multiwell. After 1-h incubation with reagent, the supernatant was removed and replaced with 100 μL dimethyl sulfoxide. Optical density at $\lambda = 570$ nm for each well sample was measured by using a microplate spectrophotometer reader (Titertek Multiskan; Flow Laboratories, Helsinki, Finland).

2.2.4 *Western blot analysis*

FTC-133 and 8305C thyroid cancer cells untreated or treated with berberine hydrochloride were harvested in cold phosphate-buffered saline (PBS), collected by centrifugation, and resuspended in a homogenizing buffer with 50-mM Tris-HCl (pH 6.8), 150-mM NaCl, 1-mM EDTA, 0.1-mM phenylmethylsulfonyl fluoride (PMSF; Sigma, Milan, Italy), and 10 μg/mL of aprotinin, leupeptin, and pepstatin. After that cells were sonicated on ice[30–32] and protein concentration of the homogenates was rapidly diluted to 1 mg/mL with reducing stop buffer (0.25M Tris-HCl, 5 mM EGTA, 25 mM dithiothreitol, 2% SDS, and 10% glycerol with bromophenol blue as dye).[21,29,30,32] Proteins were separated on 10% SDS–polyacrylamide gels and transferred to nitrocellulose membranes. Blots were blocked overnight at 4°C with 5% nonfat dry milk dissolved in 20-mM Tris–HCl, pH 7.4, 150 mM NaCl, 0.5% Tween 20. Caspase-3, p53, p27, and β-tubulin antigens were detected by 1-h incubation with mouse monoclonal antibodies against caspase-3, p53, p27, and β-tubulin (1:1,000 in PBS), respectively. The expression of each protein was visualized by chemiluminescence (ECL) kit after autoradiography film exposure. Blots were then scanned and quantified with an AlphaImager 1200 System (Alpha Innotech, San Leandro, CA). Densitometric analysis was performed after normalization with anti-mouse β-tubulin.

2.2.5 *TUNEL test*

The ApoAlert DNA fragmentation assay kit for detecting nuclear DNA fragmentation, a hallmark of apoptosis, was used. The ApoAlert DNA fragmentation assay incorporates fluorescein-dUTP at the free 3'-hydroxyl ends of the fragmented DNA and TUNEL assay was performed according to the user's manual. Cells were directly mounted and visualized by fluorescence microscopy (Leika, Germany) with either a propidium iodide (PI) filter alone or a fluorescein isothiocyanate (FITC)

filter alone. According to the user's manual, apoptotic cells appeared green with the FITC filter alone while nonapoptotic cells appeared red under the dual-pass FITC/PI filter set. We focused on 10-random microscopic fields for each dish. In each microscopic field, the number of apoptotic cells was counted and this number was compared with the number of all nonapoptotic cells visualized in the same microscopic field. The ratio was expressed as a percentage.

2.2.6 *Statistical analysis*

Data were statistically analyzed by using one-way analysis of variance (one-way ANOVA) followed by post hoc Holm–Sidak test to estimate the significant differences among groups. Data were reported as mean ± standard deviation of four experiments in duplicate, and differences between groups were considered to be significant at $*p < 0.05$.

2.2.7 *Delayed luminescence spectroscopy*

In order to perform DL measurements on untreated (control) and berberine hydrochloride treated cells, the medium was removed, the cells were washed in PBS three times and then suspended in 0.05% trypsin and 0.53 mM EDTA solution for 5 min at 37°C in humidified 5% CO_2–95% air mixture. Trypsinization was stopped by adding to the cell cultures 20% FBS, and the cells were centrifuged at 200 × g for 10 min. Pellets were suspended in PBS at room temperature (cell concentration about 10^6 cells/mL) and immediately analyzed by DL spectroscopy, by using a drop (drop volume 20 μl) from each cell line cultures, at room temperature (20 ± 1°C).

DL measurements were performed with the highly sensitive equipment able to detect single photons developed at the National Southern Laboratories of the National Nuclear Physics Institute (LNS-INFN),[33,34] and improved with a novel sample holder designed and created[35] to perform measurements on small quantity of cell cultures and to reduce possible unwanted background signals. The cell samples were illuminated by a nitrogen laser beam (Laser Photonics LN 230C; wavelength 337 nm, pulse width 5 ns, energy 100 ± 5 μJ/pulse). Photoemission signals were detected by a multialkali photomultiplier tube (Hamamatsu R-7602-1/Q) operating in single photon counting mode, with spectral range 400 to 800 nm. To reduce dark current, the photomultiplier was cooled down to −20°C. Detected signals were acquired by a multichannel scaler (Ortec MCS PCI) with a minimum dwell time of 200 ns. An electronic control of the photomultiplier gate prevented the dimpling of the photomultiplier during sample irradiation, letting the photon counting start only a few microseconds after the switching-off of the excitation pulse. Photoemission was recorded between 10 μs and 10 ms after laser excitation.

Spectra determinations were performed by filtering the light emitted by the sample by using, due to the low level of the signal, two broadband (about 80-nm FWHM) interferential filters (Lot-Oriel). More precisely, a Thermo–Oriel 57530 filter, whose maximum transmittance was at a wavelength of 460 nm (blue component), and a Thermo–Oriel 57610 filter, whose maximum transmittance was at a wavelength of 650 nm (red component), were used. Therefore, for each drop of a cell sample three measurements were performed, corresponding to the total (VIS, 400 to 800 nm), blue (460 nm) and red (650 nm) emission. DL measurements were repeated on at least five different drops from the same cells sample. Raw data of each measurement were accumulated into 50,000 acquisition channels of the multichannel scaler with a dwell time of 2 μs. At the end of the acquiring interval, the intensity of the emitted luminescence was comparable with background value. The counts of 100 repetitions of the same run were added, with a laser repetition rate of 1 Hz. To reduce random noise, a standard smoothing procedure[36] was used, by sampling the experimental points (channel values) in such a way that final data resulted in an equally spaced logarithmic time axis. The kinetics of DL intensity $I(t)$, both for the spectral components (blue and red) and the total emission (VIS), showed a multimodal behavior and DL photoemission curves could be accorded to a suitable sum of exponential time decays. Such analysis led to determine three regions for the time decay constants, namely the time intervals 10 to 100 μs, 100 μs to 1 ms and 1 to 10 ms), respectively. To facilitate comparison between different spectral DL components, which exhibited some significant differences in emission kinetics, the DL yield, that is the total number of photon emitted in the recording time interval, was calculated in the above-mentioned time domains of the DL emission, corresponding to three main classes of light emitting states, DL_1 (10 to 100 μs), DL_2 (100 μs to 1 ms) and DL_3 (1 to 10 ms) states. More precisely, at each run the ratio of the DL yield of the two spectral components (blue or red) to the total emission (VIS) was evaluated. Such a ratio is a dimensionless function, as those largely used in the literature,[4] that allows one to compare data from different samples irrespective of experimental parameters that can change from one run to the other, as cell density. Final data are reported as average value ± standard error of at least 15 different runs.

3 Results

3.1 *Effect of berberine on cellular viability of Thyroid Cancer Cell Lines*

In preliminary experiments, FTC-133 and 8305C cell line cultures were exposed to different concentrations (5 to 100 μg/mL) of berberine hydrochloride for 12, 24, or 48 h, in order to establish the optimal concentration and exposure time. The results obtained by MTT assay showed that the effect of berberine treatment strongly depended on the dose and duration of the cells' treatments. Furthermore, we found that 8305C cell lines were more resistant to berberine treatment than FTC-133 cell lines (Tables 1 and 2). Therefore, we chose to expose both cell lines to 50 μg/mL berberine hydrochloride for 24-h incubation time, because this treatment caused the smallest difference between cell survival for the two cell types.

3.2 *Effect of Berberine on the Apoptotic Pathway of Thyroid Cancer Cell Lines*

To assess the apoptotic pathway, caspase-3 cleavage by Western blot analysis and DNA fragmentation by TUNEL test was evaluated.

Figure 1 shows a representative immunoblot and densitometric analysis for the expression of caspase-3 cleavage detected on total cellular lysate of FTC-133 and 8305C cancer cell lines, both untreated and treated with 50 μg/mL of berberine for 24 h. Results showed an enhancement of caspase-3 cleavage in both cell lines treated with the alkaloid, when compared with the untreated ones, even if the effect appeared more significant

Table 1 Cell viability of FTC-133 human thyroid cancer cell lines in untreated and berberine hydrochloride treated cells at different concentrations (5 to 100 μg/mL) for 12, 24, or 48 h. Values are mean ± S.D. of four experiments in duplicate.

Cell viability (%)			
	Incubation time		
Treatment	24 h	48 h	72 h
Control	98 ± 1	99 ± 1	97 ± 1
Berberine 10 μg/mL	63 ± 2*	62 ± 1*	62 ± 3*
Berberine 25 μg/mL	37 ± 1*	36 ± 2*	35 ± 2*
Berberine 50 μg/mL	22 ± 3*	16 ± 1**	13 ± 2**
Berberine 100 μg/mL	4 ± 1*	2 ± 1**	1 ± 1**

*$p < 0.01$, significant differences versus control,
**$p < 0.05$, significant differences versus control and incubation time.

in FTC-133 cell lines [Fig. 1(a)]. Densitometric analysis of caspase-3 cleavage is reported in Fig. 1(b).

Figure 2 shows the TUNEL tests for the two types of cells, untreated and treated with 50 μg/mL of berberine for 24 h. A significant increase of DNA fragmentation in treated cells, when compared with the corresponding control samples, was found. Results of Fig. 1(b), along with data of Table 3 where a slight difference in the percentage of apoptotic cells in the two cell lines was reported, indicate that the effect of berberine was more enhanced in the follicular FTC-133 cell lines with respect to the 8305C cell lines.

3.3 *Effect of Berberine on p53 and p27 Expressions*

The effect of berberine on cell cycle regulators was evaluated. In particular, the expression of p53 and p27 on total cellular lysates from untreated and 50 μg/mL berberine treated FTC-133 or 8305C cancer cell lines was assessed. Figure 3 shows the representative immunoblots [Fig. 3(a)] and densitometric analysis for p53 [Fig. 3(b)] and p27 [Fig. 3(c)] expressions. berberine treatment induced a significant increase of p53 expression in both thyroid cancer cell lines, when compared with the respective control samples. Overexpression of p53 and p27 proteins was more evident in FTC-133 with respect to 8305C cell lines.

Table 2 Cell viability of 8305C human thyroid cancer cell lines in untreated and berberine hydrochloride treated cells at different concentrations (5 to 100 μg/mL) for 12, 24, or 48 h. Values are mean ± S.D. of four experiments in duplicate.

Cell viability (%)			
	Incubation time		
Treatment	24 h	48 h	72 h
Control	97 ± 1	99 ± 1	98 ± 1
Berberine 10 μg/mL	78 ± 1*	64 ± 1**	63 ± 3**
Berberine 25 μg/mL	66 ± 3*	54 ± 2**	35 ± 2**
Berberine 50 μg/mL	23 ± 2*	9 ± 1**	4 ± 1**
Berberine 100 μg/mL	20 ± 1*	5 ± 1**	3 ± 1**

*$p < 0.01$, significant differences versus control.
**$p < 0.05$, significant differences versus control and incubation time.

3.4 *Delayed Luminescence Measurements to Monitor the Effect of Berberine Treatment in Thyroid Cancer Cell Lines*

As it regards DL measurements, in addition to the DL intensity emitted in the total wavelength range of the detection apparatus (VIS component, 400 to 800 nm), we measured only two spectral components (see Sec. 2.2.7), the blue component (λ_{em} = 460 nm), likely related to NADH emission, and the red component (λ_{em} = 645 nm), likely related to PpIX emission. Due to the fact that in our experimental apparatus spectral measurements can be only sequentially performed, in order to shorten the duration of each measurement, so preventing cell stress, we limited the spectral analysis only to these two components.

The first analysis was performed by considering the total number of photons emitted in the whole time interval of measurement. More precisely, to compare the DL response, we evaluated the ratio of each of the spectral components to the emission in the whole wavelength range, in order to have parameters that do not depend on cell densities. Figure 4 reports the percentage of each spectral component for the two cells types, untreated and treated with 50 μg/mL of berberine hydrochloride for 24 h. After the treatment DL total emission from each of the two cell lines decreased with respect to the control samples, but the spectral response of the two cell lines was different. In the anaplastic cells, the blue component was the largest part of the total emission and the one affected by berberine, while in the differentiated follicular cells the red component was the largest part and the one affected by berberine. Changes in the other components were inside the error in both cases.

Figure 5 reports the typical temporal DL trends for the two different cell lines. The total and the two above-mentioned spectral components are reported for untreated (control) samples. The same features in DL trends were observed after berberine treatment. The multimodal behavior of DL, previously observed in other cell lines,[5,7,27,28] is evident. As described in Sec. 2.2.7, in order to take such multimodal behavior of DL and facilitate comparison between different spectral DL components into account, the DL yield was calculated in the three time domains of the DL emission, corresponding to three main classes of light emitting states, DL_1 (10 to 100 μs), DL_2 (100 μs to 1 ms) and DL_3 (1 to 10 ms) states.

Figures 6 and 7 respectively report the percentage of the blue (Fig. 6) and red (Fig. 7) components with respect to the total (VIS) emission for the three classes of light emitting states. Untreated and berberine hydrochloride treated human thyroid follicular FTC-133 [Figs. 6(a) and 7(a)] and anaplastic 8305C cell lines [Figs. 6(b) and 7(b)] are compared. It appears that in the anaplastic cells, the blue component was the largest fraction of the total emission [see Fig. 4(b)] and there was a strong reduction of this component after berberine treatment all over the time course of the decay [see Fig. 6(b)], while in the well-differentiated follicular cells a decrease of the blue component occurred only at long time [see Fig. 6(a)]. Moreover, in the case of follicular cells, the predominance of the red component with respect to the blue one, as well as its decrease after berberine treatment [see Fig. 4(a)], actually

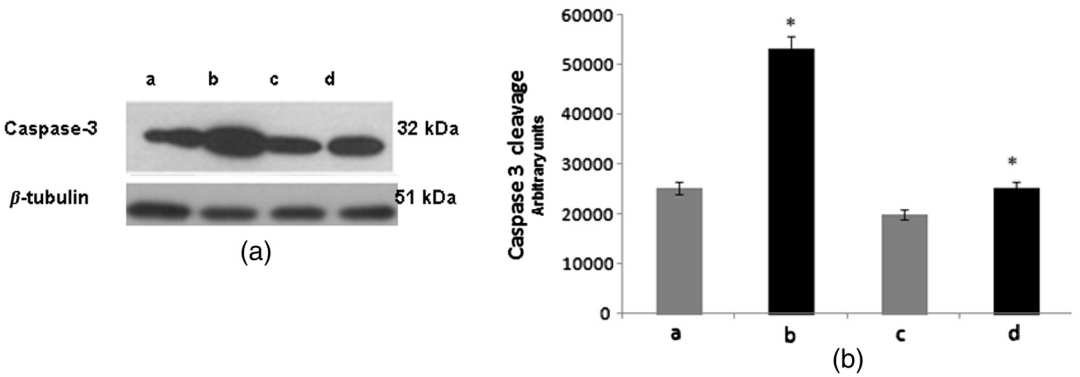

Fig. 1 (a) Representative immunoblot of caspase-3 cleavage in untreated and 50 μg/mL berberine hydrochloride treated for 24-h FTC-133 and 8305C human thyroid cancer cell lines. (b) Densitometric analysis of caspase-3 cleavage (performed after normalization with β-Tubulin) in response to treatment with berberine: results are expressed as mean $\pm$ SD of the values of four experiments in duplicate. $^*p < 0.05$, significant differences versus control and berberine treated cells. (a) Untreated FTC-133 cell line cultures; (b) FTC-133 cell line cultures treated with 50 μg/mL berberine hydrochloride for 24 h; (c) untreated 8305C cell line cultures; (d) 8305C cell line cultures treated with 50 μg/mL berberine hydrochloride for 24 h.

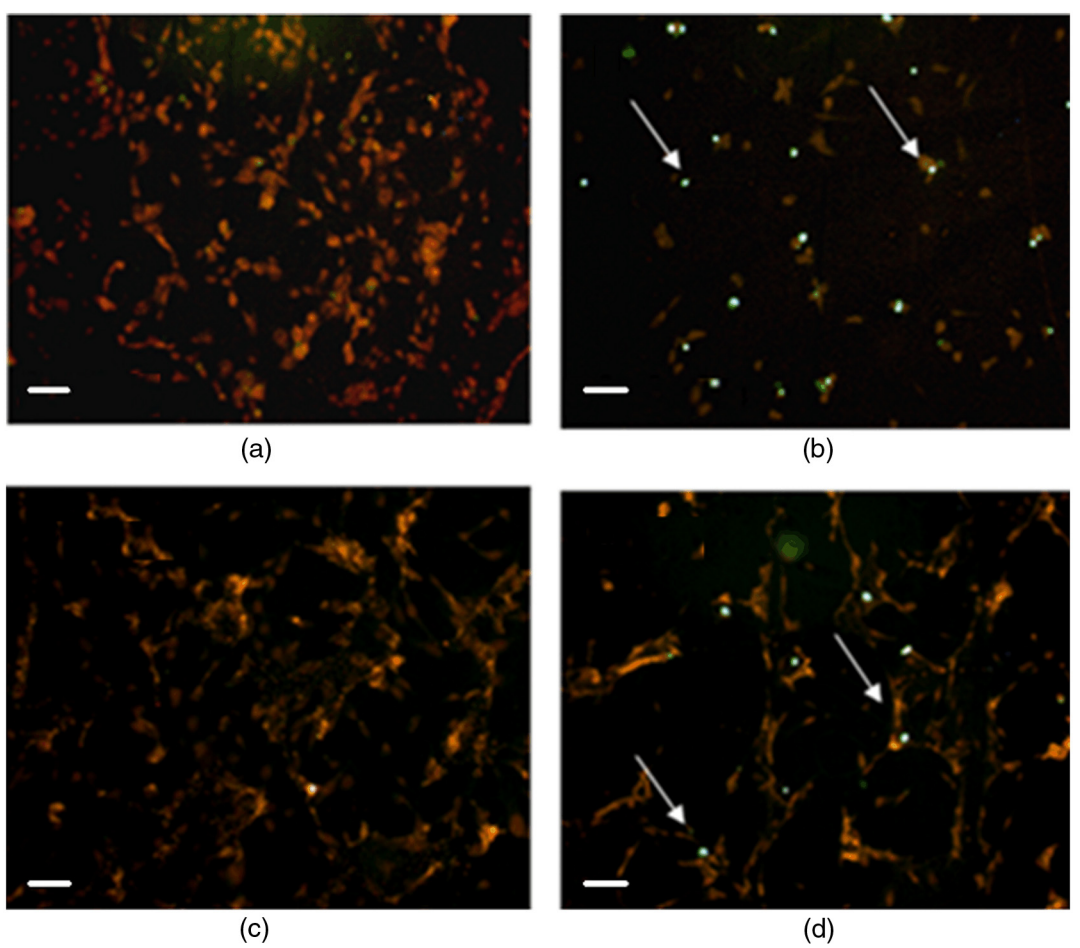

Fig. 2 Representative pictures of TUNEL test performed on untreated and 50 μg/mL berberine hydrochloride treated for 24-h FTC-133 and 8305C human thyroid cancer cell lines: immunostaining of non-apoptotic (red) and apoptotic (green) cells is shown (scale bars = 20 μm). (a) untreated FTC-133 cell line cultures; (b) FTC-133 cell line cultures treated with 50 μg/mL berberine hydrochloride for 24 h; (c) untreated 8305C cell line cultures; (d) 8305C cell line cultures treated with 50 μg/mL berberine hydrochloride for 24 h.

Table 3 Percentage of apoptotic cells in follicular (FTC-133) and anaplastic (8305C) human thyroid cancer cell lines treated with 50 μg/mL berberine hydrochloride for 24 h, as evaluated by TUNEL test. Values are mean $\pm$ SD of 10 random microscopic fields for each dish.

	Percentage of apoptotic cells	
Treatment	FTC-133	8305C
Control	3 ± 1	2 ± 1
Berberine 50 μg/mL	93 ± 3	87 ± 2

occurred only in the short time region [see Fig. 7(a)], with significant difference at $p < 0.06$.

4 Discussion

We investigated the correlation between apoptosis induced by berberine treatments and UVA-induced DL from two human thyroid cancer cell lines, FTC-133 and 8305C, as representative of follicular and anaplastic thyroid human cancers, respectively. In fact, recent advances have shown that berberine exerts anticancer activities both *in vitro* and *in vivo* through different mechanisms, which underlie its anti-proliferative and proapoptotic effects.[25,37–39]

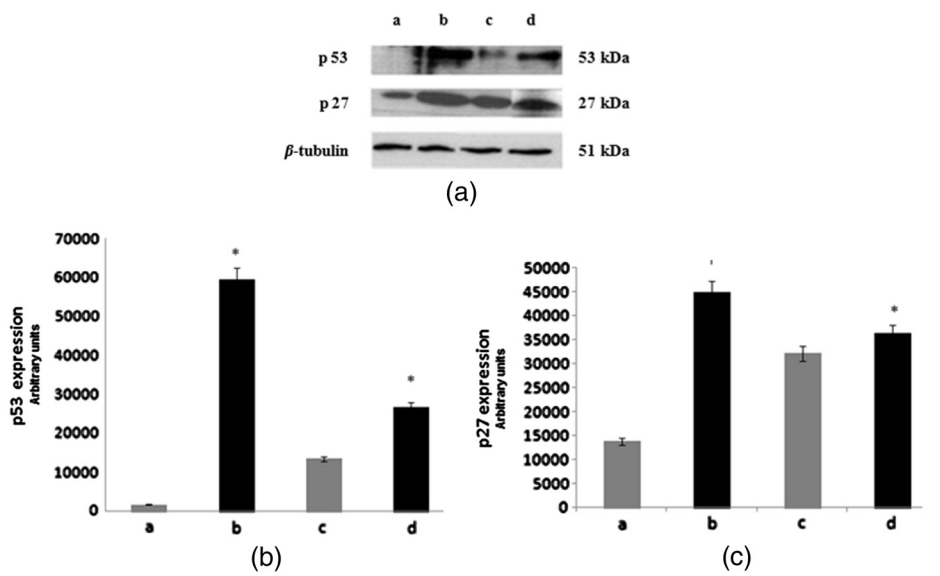

Fig. 3 (a) Representative immunoblots of p53 and p27 expressions in untreated and 50 μg/mL berberine hydrochloride treated for 24-h FTC-133 and 8305C human thyroid cancer cell lines. (b) Densitometric analysis of p53 and p27 (performed after normalization with β-Tubulin) in response to treatment with berberine: results are expressed as mean $\pm$ SD of the values of four experiments in duplicate. $^*p < 0.05$, significant differences versus control and berberine treated cells. (a) Untreated FTC-133 cell line cultures; (b) FTC-133 cell line cultures treated with 50 μg/mL berberine hydrochloride for 24 h; (c) untreated 8305C cell line cultures; (d) 8305C cell line cultures treated with 50 μg/mL berberine hydrochloride for 24 h.

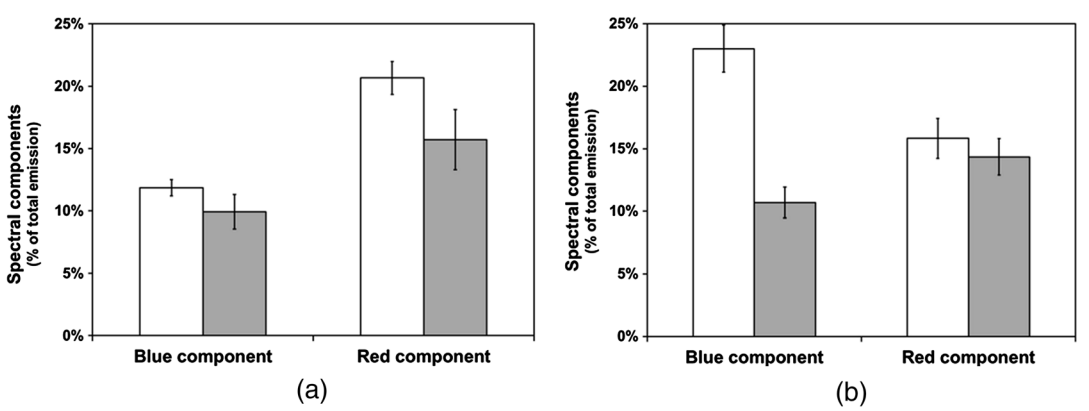

Fig. 4 Spectral components percentage of DL emission from untreated (white bars) and 50 μg/mL berberine hydrochloride for 24-h treated (gray bars) cell lines for the blue component ($\lambda_{em} = 460$ nm) and the red component ($\lambda_{em} = 645$ nm). (a) Follicular FTC-133 cell line, (b) anaplastic 8305C cell line. Results are expressed as average $\pm$ SE values of three different experiments in quintuplicate.

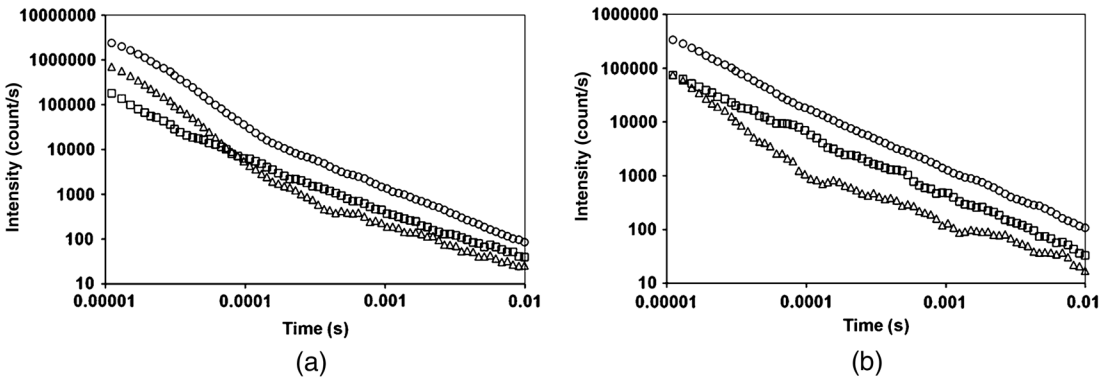

Fig. 5 Typical temporal decay of DL from (a) FTC-133 and (b) 8305C human thyroid cancer cell lines. (Circle) VIS (400-800 nm), (square) blue ($\lambda_{em} = 460$ nm) and (triangle) red ($\lambda_{em} = 645$ nm) components.

The anticancer effect of berberine was evaluated through the examination of cell cycle and apoptosis modulation. Our data showed that berberine treatment of human thyroid cancer cell lines is able to arrest cell cycle, also activating the apoptotic pathway, as shown in both cell lines by the increase of caspase-3 cleavage, DNA fragmentation, and p53 and p27 proteins overexpression. In particular, p53 and p27 are typically implicated in the arrest of cell cycle or in its slowing down. The effect of berberine treatment on the cells appeared more evident in follicular thyroid FT-133 cell lines. The difference between the extents of such an effect in the two cell lines is consistent with the different tumorigenic grade of FTC-133 cells, representative of slow growing well-differentiated cancer cell lines, with respect to 8305C cells, representative of rapid proliferating high de-differentiated thyroid cancer cell lines. Consistently, our results demonstrate that berberine inhibits thyroid cancer cell growth through cell-cycle block, and suggests that it can be a novel candidate for anti-cancer agent against thyroid cancer.

Several effects on cancer cell lines described in the literature have been attributed to berberine effects on mitochondria, including inhibition of mitochondrial Complex I and interaction with the adenine nucleotide translocator.[26,40,41] The mitochondrial origin of the DL signal was moreover hypothesized in studying the response of human leukemia cells to proapoptotic treatments.[27,28]

We have examined two spectral components of DL emission spectrum, the blue component ($\lambda_{em} = 460$ nm) and the red component ($\lambda_{em} = 645$ nm). Likely, candidates for the observed spectral components of the DL emission are reduced nicotinamide adenine dinucleotide (NADH) and protoporphyrin IX (PpIX), a heme precursor, respectively.

It is known that NADH is an essential cofactor for oxidation-reduction (redox) reactions and energy metabolism in living cells. In the electron transport chain of the inner membrane of mitochondria, NADH (fluorescent) is oxidized to NAD+ (not fluorescent), which eventually leads to the majority of adenosine triphosphate (ATP) production via the oxidative phosphorylation pathway. Concentration and distribution of intrinsic NADH in living cells are sensitive to cell physiology and pathology. As a result, there is a great potential for cellular NADH as a natural biomarker for a range of cellular processes such as apoptosis, redox reactions, and mitochondrial anomalies associated with cancer and neurodegenerative diseases. In particular, NADH concentration in cancer cells was estimated higher than in normal cells.[8] Moreover, the ratio of NADH to flavin adenine dinucleotide (FAD) was used to differentiate cancerous from noncancerous tissues in a variety of models including oral and breast cancer, being a measurement of the balance between glycolysis (seen in tumor cells) and oxidative phosphorylation (seen in untransformed cells).[12]

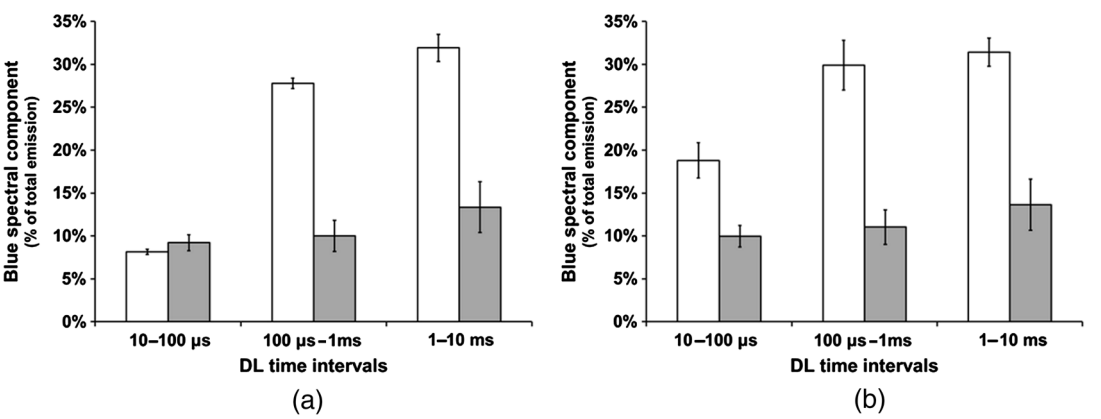

Fig. 6 Blue component ($\lambda_{em} = 460$ nm) percentage of DL emission from cell lines in different time intervals of the temporal decay. Untreated (white bars) and 50 μg/mL berberine hydrochloride for 24-h treated (gray bars) human thyroid cancer cells. (a) FTC-133 cell line, (b) 8305C cell line. Results are expressed as average $\pm$ SE values of three different experiments in quintuplicate.

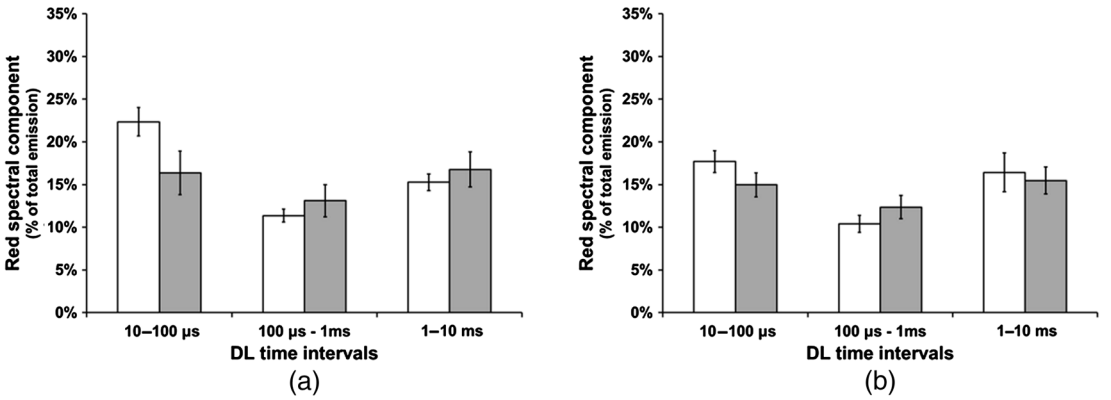

Fig. 7 Red component ($\lambda_{em} = 645$ nm) percentage of DL emission from cell lines in different time intervals of the temporal decay. Untreated (white bars) and 50 μg/mL berberine hydrochloride for 24-h treated (gray bars) human thyroid cancer cells. (a) FTC-133 cell line, (b) 8305C cell line. Results are expressed as average ± SE values of three different experiments in quintuplicate.

On the other hand, increased concentrations of porphyrin and FAD were observed in cancerous tissues as compared to normal ones,[13] and an additional presence of autofluorescence emission in the red region, ascribed to PpIX, was recurrently reported in the case of neoplastic tissues.[10] Moreover, interaction of PpIX with the p53 tumor suppressor protein, showing activation of its proapoptotic activity, was investigated in the view of using photodynamic therapy of cancer as an alternative treatment of tumor resistant to chemo- and radiotherapy,[14] and delayed fluorescence of PpIX, after application of its precursor 5-aminolevulinic acid hydrochloride (ALA) was used for *in vivo* measurements of mitochondrial oxygen tension.[15–17]

The obtained results, reported in Figs. 4–7, show that the two different cell types have a different spectral response in their native state, which is before any treatments. Differentiated follicular FTC-133 cells show a predominance of the red component in their DL spectrum, while in anaplastic 8305C cells, the blue component is the largest fraction of the total emission. According to the above cited literature, one possible explanation of the greater red component in FTC-133 cells than in 8305C cells could be related to iron homeostasis. In fact, while in the anaplastic 8305C cells, increased iron requirement is related to the intensive angionesis, in the differentiated FTC-133 cells a relevant iron uptake is required for aerobic mitochondrial respiration. Therefore, the increased PpIX emission in differentiated cells could be interpreted according to an inability to complete the heme synthesis in mitochondria because of iron shortage, confirming also the mitochondrial nature of the DL signal.

Our hypothesis is supported by other preliminary results relative to the expression of transferrin receptor 1 (TfR1), which represents the major mediator of iron uptake by cells, showing a larger overexpression in anaplastic 8305C cells when compared with the follicular FTC-133 cell lines, and a prevalent localization of TfR1 in mitochondria of follicular cell lines.

As it regards the spectral response after berberine treatment (Figs. 4, 6, and 7), the reduction of the red component observed in FTC-133 cells [Fig. 4(a)], that actually occurs at short times of the decay [Fig. 7(a)], could be related to the antioxidant effect of berberine: the idea is that acting with a SOD mimic mechanism berberine could favor the dismutation of superoxide and so increasing oxygen levels, which results in an enhancing of DL quenching (and consequent DL decrease) from PpIX.[15] On the other side, the reduction of the blue component, all over the time course of the decay for the anaplastic 8305C cells [Fig. 6(b)] and at a long time in the well-differentiated follicular FTC-133 cells [Fig. 6(a)], is similar to what observed in the paper of Baran et al.[27] as an effect of the bioflavonoid quercetin on DL from leukemia human T-cells, where this reduction was linked to NADH oxidation and an irreversible decrease of intramitochondrial NADH pool. This is consistent with caspase activation of the apoptotic pathway (and consequent ATP decrease) through the release of cytochrome *c* as a result of the outer mitochondrial membrane becoming permeable. Therefore, in agreement with the results obtained for other cells type,[7,27,28] the strong variation of the blue component, especially at longer times, seems to be a hallmark of induced apoptosis.

5 Conclusions

Our findings show that berberine treatment of thyroid cancer cell lines is able to arrest cell cycle and activate apoptotic pathway as shown in both cell lines by DNA fragmentation, caspase-3 cleavage, p53 and p27 proteins overexpression. In parallel, changes in DL spectral components after berberine treatment support the hypothesis that DL from human cells originates mainly from mitochondria, since berberine acts especially at the mitochondrial level.

In addition, the strong decrease of the DL blue component for both cell lines may be a hallmark of induced apoptosis, while the different response in the red spectral range may be ascribed to a different iron homeostasis in the two cell lines.

The results encourage further studies toward the use of DL spectroscopy in clinical applications as a valuable investigation tool in a multiparameters approach to cancer diagnosis and monitoring of therapeutic treatments.

Acknowledgments

The research was supported by Italian Ministry of University and Research (MIUR) as Project No. 2008XAWB9H in the frame of Research Projects of National Interest (PRIN).

References

1. M. Takeda et al., "A novel method of assessing carcinoma cell proliferation by biophoton emission," *Cancer Lett.* **127**(1–2), 155–160 (1998).

2. L. Lanzanò et al., "Spectral analysis of delayed luminescence from human skin as a possible non-invasive diagnostic tool," *Eur. Biophys. J. Biophys. Lett.* **36**(7), 823–829 (2007).
3. H. J. Niggli et al., "Laser-Ultraviolet-A induced ultraweak photon emission in mammalian cells," *J. Biomed. Opt.* **10**(2), 024006 (2005).
4. F. Musumeci et al., "Spectral analysis of laser-induced ultraweak delayed luminescence in cultured normal and tumor cells: temperature dependence," *J. Photochem. Photobiol. B-Biol.* **79**(2), 93–99 (2005).
5. F. Musumeci et al., "Discrimination between normal and cancer cells by using spectral analysis of delayed luminescence," *Appl. Phys. Lett.* **86**(15), 153902 (2005).
6. H-W. Kim et al., "Spontaneous photon emission and delayed luminescence of two types of human lung cancer tissues: adenocarcinoma and squamous cell carcinoma," *Cancer Lett.* **229**(2), 283–289 (2005).
7. I. Baran et al., "Effects of menadione, hydrogen peroxide and quercetin on apoptosis and delayed luminescence of human leukemia Jurkat T-cells," *Cell Biochem. Biophys.* **58**(3), 169–179 (2010).
8. H. Andersson et al., "Autofluorescence of living cells," *J. Microsc.* **191**(1), 1–7 (1998).
9. A. C. Croce et al., "Dependence of fibroblast autofluorescence properties on normal and transformed conditions. Role of the metabolic activity," *Photochem. Photobiol.* **69**(3), 364–374 (1999).
10. A. C. Croce et al., "Naturally-occurring porphyrins in a spontaneous-tumor bearing mouse model," *Photochem. Photobiol. Sci.* **10**(7), 1189–1195 (2011).
11. Q. Yu and A. A. Heikal, "Two-photon autofluorescence dynamics imaging reveals sensitivity of intracellular NADH concentration and conformation to cell physiology at the single-cell level," *J. Photochem. Photobiol. B-Biol.* **95**(1), 46–57 (2009).
12. A. Walsh et al., "Optical imaging of metabolism in HER2 overexpressing breast cancer cells," *Biomed. Opt. Express* **3**(1), 78–85 (2012).
13. S. Kala et al., "Optical spectroscopy: a promising diagnostic tool for breast lesions," *J. Clin. Diagn. Res.* **5**(8), 1574–1577 (2011).
14. J. Zawacka-Pankau et al., "Protoporphyrin IX interacts with wild-type p53 protein in vitro and induces cell death of human colon cancer cells in a p53-dependent and -independent manner," *J. Biol. Chem.* **282**(4), 2466–2472 (2007).
15. E. G. Mik et al., "Mitochondrial PO_2 measured by delayed fluorescence of endogenous protoporphyrin IX," *Nat. Methods* **3**(11), 939–945 (2006).
16. E. G. Mik et al., "*In vivo* mitochondrial oxygen tension measured by a delayed fluorescence lifetime technique," *Biophys. J.* **95**(8), 3977–3990 (2008).
17. F. A. Harms et al., "Oxygen-dependent delayed fluorescence measured in skin after topical application of 5-aminolevulinic acid," *J. Biophotonics* **4**(10), 731–739 (2011).
18. S. Elmore, "Apoptosis: a review of programmed cell death," *Toxicol. Pathol.* **35**, 495–516 (2007).
19. S. Desagher and J.-C. Martinou, "Mitochondria as the central control point of apoptosis," *Trends Cell. Biol.* **10**(9), 369–377 (2000).
20. R. Musumeci et al., "*Berberis aetnensis* C. Presl. extracts: antimicrobial properties and interaction with ciprofloxacin," *Int. J. Antimicrob. Agents* **22**(1), 48–53 (2003).
21. A. Campisi et al., "Effect of berberine and *Berberis aetnensis* C. Presl. alkaloid extract on glutamate-evoked tissue transglutaminase up-regulation in astroglial cell cultures," *Phytother. Res.* **25**(6), 816–820 (2011).
22. J. M. Hwang et al., "Berberine induces apoptosis through a mitochondria/caspases pathway in human hepatoma cells," *Arch. Toxicol.* **80**(2), 62–73 (2006).
23. J. P. Lin et al., "Berberine induces cell cycle arrest and apoptosis in human gastric carcinoma SNU-5 cell line," *World J. Gastroenterol.* **12**(1), 21–28 (2006).
24. K. Yan et al., "Induction of G1 cell cycle arrest and apoptosis by berberine in bladder cancer cells," *Eur. J. Pharmacol.* **661**(1–3), 1–7 (2011).
25. K. S. Park et al., "Berberine inhibited the growth of thyroid cancer cell lines 8505C and TPC1," *Yonsei Med. J.* **53**(2), 346–351 (2012).
26. G. C. Pereira et al., "Mitochondrially targeted effects of berberine [Natural Yellow 18, 5,6-dihydro-9,10-dimethoxybenzo(g)-1,3-benzodioxolo(5,6-a) quinolizinium] on K1735-M2 mouse melanoma cells: comparison with direct effects on isolated mitochondrial fractions," *J. Pharmacol. Exp. Ther.* **323**(2), 636–49 (2007).
27. I. Baran et al., "Detailed analysis of apoptosis and delayed luminescence of human leukemia Jurkat Tcells after proton-irradiation and treatments with oxidant agents and flavonoids," *Oxid. Med. Cell. Longev.* **2012**, 498914 (2012).
28. I. Baran et al., "Mitochondrial respiratory complex I probed by delayed luminescence spectroscopy," *J. Biomed. Opt.* **18**(12), 127006 (2013).
29. A. Campisi et al., "Glutamate-induced increases in transglutaminase activity in primary cultures of astroglial cells," *Brain Res.* **978**(1–2), 24–30 (2003).
30. A. Campisi et al., "Glutamate-evoked redox state alterations are involved in tissue transglutaminase upregulation in primary astrocyte cultures," *FEBS Lett.* **578**(1–2), 80–84 (2004).
31. A. Campisi et al., "Effect of growth factors and steroids on transglutaminase activity and expression in primary astroglial cell cultures," *J. Neurosci. Res.* **86**(6), 1297–1305 (2008).
32. A. Campisi et al., "Expression of tissue transglutaminase on primary olfactory ensheathing cells cultures exposed to stress conditions," *Neurosci. Res.* **72**(4), 289–295 (2012).
33. S. Tudisco et al., "Advanced research equipment for fast ultraweak luminescence analysis," *Rev. Sci. Instrum.* **74**(10), 4485–4490 (2003).
34. S. Tudisco et al., "ARETUSA-Advanced research equipment for fast ultraweak luminescence analysis: new developments," *Nucl. Instrum. Methods Phys. Res. Sect. A-Accel. Spectrom. Dect. Assoc. Equip.* **518**(1–2), 463–464 (2004).
35. A. Scordino et al., "Ultra-weak delayed luminescence in cancer research: a review of the results by the ARETUSA equipment," *J. Photochem. Photobiol. B-Biol.* **139**, 76–84 (2014).
36. A. Scordino et al., "Influence of the presence of atrazine in water on the in vivo delayed luminescence of Acetabularia acetabulum," *J. Photochem. Photobiol. B-Biol.* **32**(1–2), 11–17 (1996).
37. Y. Sun et al., "A systematic review of the anticancer properties of berberine, a natural product from Chinese herbs," *Anticancer Drugs* **20**(9), 757–769 (2009).
38. W. Tan et al., "Berberine hydrochloride: anticancer activity and nanoparticulate delivery system," *Int. J. Nanomed.* **6**, 1773–1777 (2011).
39. S. Letasiová et al., "Berberine-antiproliferative activity in vitro and induction of apoptosis/necrosis of the U937 and B16 cells," *Cancer Lett.* **239**(2), 254–262 (2006).
40. C. V. Diogo et al., "Berberine as a promising safe anti-cancer agent—is there a role for mitochondria?," *Curr. Drug Targets* **12**(6), 850–859 (2011).
41. C. V. Pereira, N. G. Machado, and P. J. Oliveira, "Mechanisms of berberine (natural yellow18)-induced mitochondrial dysfunction: interaction with the adenine nucleotide translocator," *Toxicol. Sci.* **105**(2), 408–417 (2008).

Agata Scordino is an associate professor of experimental physics at the University of Catania, Italy, where she received her degree in physics in 1980. She is the author of more than 130 papers in international journals and scientific books. Her current scientific interests include spontaneous and photo-induced ultraweak photon emission from living systems and development of innovative instrumentation for photon detection. She has collaborated with researchers from Italy, the Netherlands, Poland, Romania, Switzerland, United Kingdom, and Ukraine.

Agata Campisi is an associate professor of biochemistry in the Pharmaceutical Sciences Department at the University of Catania. She is the author of more than 160 publications, including articles in international journals, book chapters, and conference proceedings. Her current scientific interests include neurodegeneration/neuroprotection, apoptosis, cell signaling, cancer biomarkers, and drug delivery.

Rosaria Grasso received her degree in electronic engineering in 2005 and received her PhD degree in physical engineering cum laude in 2009 at the University of Catania, Italy. She has worked on detection of ultraweak induced photon emission from biological systems and the study, design, and testing of detectors for time-resolved imaging with single-photon sensitivity. She also investigated the nonthermal effect induced by radio frequency electromagnetic fields on cell cultures.

Roberta Bonfanti received her master's degree in cellular and molecular biology in 2009, and received her PhD degree in microbiological and biochemical sciences in 2014, at the University of Catania,

Italy. Her current scientific interests include neurodegeneration/neuroprotection, apoptosis, cell signaling, cancer biomarkers, and drug delivery.

Marisa Gulino is an associate professor of experimental physics at the University of Enna Kore, Italy. In 2000, she received her PhD degree in physics cum laude at the University of Catania, Italy. She has been a post-doc researcher with Katholieke Universiteit Leuven, Belgium, and a researcher at the University of Catania. She is the author of more than 100 papers in international journals. Her current scientific interests include photo-induced ultraweak photon emission from living systems and from pure water.

Liliana Iauk was associate professor of the faculty of pharmacy at the University of Catania, Italy. She started her scientific activity in 1978 in the field of medicinal plants and drugs activity. She published more than 60 scientific papers. Unfortunately, she died in December 2013.

Rosalba Parenti is an associate professor of physiology in the Biomedical Sciences Department at the University of Catania. She is the author of more than 80 publications, including articles in international journals, book chapters, and conference proceedings. Her current scientific interests include anatomo/functional organization of nervous system, neurodegeneration/neuroprotection, development, cancer biomarkers, and drug delivery.

Francesco Musumeci is a full-time professor of applied physics at the University of Catania, and has been a visiting professor at the University of Kyoto, Japan, and at the University of Washington, United States. His research activities were focused on the field of solar energy, on the interaction between electromagnetic waves and rough metal surfaces. His current research interests include the investigation of ultraweak luminescence, spontaneous and photo-induced from biological systems, and the dielectric properties of aqueous solutions.